Microporous and Mesoporous Materials 252 (2017) 29–36

Contents lists available at ScienceDirect

Microporous and Mesoporous Materials

journal homepage: www.elsevier.com/locate/micromeso

Fluoride-mediated synthesis of TON and MFI zeolites using 1-butyl-3-methylimidazolium as structure-directing agent

Christian W. Lopes [a], Luis Gómez-Hortigüela [b], Alex Rojas [c], Sibele B.C. Pergher [a, *]

[a] LABPEMOL – Universidade Federal do Rio Grande do Norte, Av. Senador Salgado Filho, 3000, 59078-970 Natal, RN, Brazil
[b] Instituto de Catálisis y Petroleoquímica, Consejo Superior de Investigaciones, Científicas (ICP-CSIC), c/Marie Curie 2, 28049 Madrid, Spain
[c] LPQA, Universidade Federal do Maranhão, Av. dos Portugueses, 1966, Bacanga, 65080-805 São Luís, MA, Brazil

ARTICLE INFO

Article history:
Received 21 April 2017
Received in revised form
3 June 2017
Accepted 8 June 2017
Available online 9 June 2017

Keywords:
Zeolite synthesis
Fluoride media
TON
MFI
Ionic liquid
1-butyl-3-methylimidazolium
Titanium

ABSTRACT

In this work, 1-butyl-3-methylimidazolium (1B3MI) cation has been employed as a structure-directing agent for the synthesis of pure silica and Ti-containing zeolites in fluoride media. The 1B3MI OSDA exhibited distinct phase selectivity depending on the synthesis conditions, and particularly the concentration of the synthesis gel. Thus, under more diluted conditions ($H_2O/SiO_2 = 14$), the 1B3MI cation yielded pure silica TON zeolite with high crystallinity. Attempts to obtain Ti-containing zeolites, however, failed at this diluted condition even after 15 days of synthesis. In contrast, highly crystalline Ti-MFI was the only phase obtained upon reducing the H_2O/SiO_2 molar ratio from 14 to 7. The presence of Ti in the MFI zeolite framework was confirmed by both infrared and DRS UV-vis spectroscopies. The presence of intact OSDA molecules within the micropores was inferred from elemental analysis and ^{13}C CP-MAS NMR spectroscopy. On the other hand, thermogravimetric analyses showed a different packing of the 1B3MI cation in the pure silica TON and Ti-MFI samples. Moreover, the environments for Si and F species in the as-made materials were investigated by means of ^{29}Si and ^{19}F MAS NMR, respectively. Finally, molecular simulations showed that the most stable arrangement of the 1B3MI cations involves the location of the imidazolium rings on the channel intersections and of the butyl chains on the sinusoidal channels.

1. Introduction

Zeolites and zeotypes are inorganic crystalline materials containing pores and channels of molecular dimensions which have found relevant applications in numerous catalytic and separation processes. Their frameworks are based on TO_4 units (where T = Si, Al, Ti, Ge, Sn, P) connected by four oxygen atoms in tetrahedral geometry. Most commonly, zeolites are synthesized under hydrothermal conditions using hydroxide anions as mineralizing agent [1,2]. However, a significant breakthrough in the field of zeolite synthesis was the development of an alternative route employing fluoride anions as mineralizing agent [3]. This methodology allowed the synthesis in neutral or even acidic conditions, enabling the use of new organic structure-directing agents (OSDAs) that otherwise would not be stable at the conditions of high pH of alkaline-mediated synthesis. Moreover, the fluoride route allows the incorporation of heteroatoms other than Si and Al in the zeolite framework which precursors would form unreactive precipitates in alkaline solutions [1]. Furthermore, this approach successfully led to the discovery of new zeolite structures [4,5]. Zeolites synthesized by the fluoride route typically display specific features, such as low (or null) concentration of connectivity defects, leading to an increased hydrophobicity, and large crystal sizes [3,6,7], both properties being of particular relevance in specific catalytic and adsorption/separation processes [1,3].

Another topic which has deserved great focus of attention in the field of zeolite synthesis is the study of different classes of organic compounds as structure-directing agents [1]. In this respect, imidazolium-based compounds have shown high potential as OSDA [8–20] due to the possibility to tune their size, shape, and flexibility by proper choice of the ligands, which make them interesting from the synthesis point of view. This class of structure-directing agents enabled the synthesis of new zeolitic materials (e.g. IM-16 [21], IM-20 [20], ITW [22], CIT-7 [23]), stabilization of already known structures (HPM-1 [15,24], ITW [17,25]) and made

* Corresponding author.

http://dx.doi.org/10.1016/j.micromeso.2017.06.017
1387-1811/

possible the synthesis of zeolites in novel compositions [10,26]. In addition, the so-called ionothermal synthesis of zeolites has been first described using imidazolium-based compounds as structure-directing agents and solvents at the same time due to their intrinsic properties (e.g. low vapor pressure and high thermal stability) [27–29]. Recently, Wen et al. [19] noted that the size of 1-butyl-3-methylimidazolium (one of the most investigated ionic liquids found in literature [30,31]) is consistent with the channel size of TON, what makes it a good candidate as structure-directing agent for this topology. Indeed, this behavior was confirmed by our group in the synthesis of TiO_2 and Al-containing TON zeolite in hydroxide media [10,11].

Following our precedent work, in the present study we have explored the synthesis of pure silica and Ti-containing zeolites (with high potential as catalysts for selective oxidations in liquid phase) by combining 1-butyl-3-methylimidazolium and fluoride anions under different conditions. In particular, the influence of the H_2O/SiO_2 molar ratio in the gel, the synthesis time, and the addition of zeolite seeds on the crystallization outcome is investigated. The chemical, structural, and morphological properties of the as-made zeolites were discussed based on different characterization techniques.

2. Experimental section

2.1. Synthesis of 1-butyl-3-methylimidazolium

1-butyl-3-methylimidazolium (1B3MI) was synthesized in the chloride form (1B3MICl) according to a published procedure [32]. In a typical reaction, 1-methylimidazole (1 mol) and 1-chlorobutane (1.1 mol) were dissolved in acetonitrile and subjected to stirring under reflux for 48 h at 80 °C. The crystallization of the product was performed by adding the 1B3MICl solution to a round-bottom flask containing ethyl acetate followed by storage of the solution in a freezer for 24 h. The resulting white solid was dried under reduced pressure until a constant weight was achieved. The product yield was 75%.

For the synthesis of zeolites, 1B3MICl was converted to the hydroxide form (1B3MIOH) by anion exchange in aqueous solution using Dowex Monosphere 550A (OH) anion exchange resin (Aldrich), following a previously reported methodology [16], resulting in a degree of exchange of 95.6%.

2.2. Synthesis of zeolites

For the synthesis of pure silica zeolites, tetraethylorthosilicate (TEOS, ≥99%, Merck) was hydrolyzed at 25 °C under stirring in an aqueous solution of 1B3MIOH. Afterwards, ethanol and water were evaporated until the desired composition (monitored by weight) was reached. Next, HF (≥40% aqueous solution, Sigma-Aldrich) was added and the mixture was stirred for 15 min. The molar composition of the gel was 1 SiO_2: 0.5 OSDA: 0.5 HF: 14 H_2O. Then, three equivalent aliquots of the gel were poured into 60 mL Teflon-lined stainless steel autoclaves and heated in an oven at 160 °C for 4, 5, and 13 days under static conditions. After the reaction period, the solids were filtered, washed with distilled water, and finally dried for 24 h at 100 °C. This synthesis will be referred as A.

Ti-containing zeolites were synthesized at 160 °C in static with a HF/SiO_2 molar ratio of 0.5 as for the pure silica samples (synthesis A) using tetraethylorthotitanate (TEOT, ~95%, Merck) as the Ti source. The mixture of TEOT and TEOS was hydrolyzed until the desired gel composition was attained. In all syntheses the Si/Ti molar ratio in the gel was kept constant at 50. In synthesis B, a small amount (2 wt%) of pure silica TON seeds (from synthesis A) was added to the synthesis mixture while keeping the H_2O/SiO_2 molar ratio at 14 as for synthesis A, and reacted for 4, 8, and 15 days. In synthesis C, the H_2O/SiO_2 molar ratio was decreased to 7. In this case, hydrogen peroxide was added to the synthesis gel (SiO_2/H_2O_2 molar ratio of 0.333) so as to prevent formation of anatase [33] which is known to decompose H_2O_2 decreasing the efficiency of the Ti-containing catalyst during the liquid phase selective oxidations [34]. In this case, the gel mixture was reacted for 18 days. Finally, the conditions for synthesis D were identical to those used in synthesis C, except that no H_2O_2 was added and that the mixture was kept reacting under hydrothermal conditions for either 13 or 31 days.

The as-synthesized zeolites are labeled as S-t, where “S” stands for the specific synthesis employed (A, B, C, or D) and “t” refers to the crystallization time (in days).

2.3. Characterization methods

The structural parameters were evaluated by X-ray diffraction in a Bruker D2 Phaser instrument using Ni-filtered CuK_α ($\lambda = 0.154$ nm) radiation, a step size of 0.02°, a current of 10 mA, a voltage of 30 kV, and a Lynxeye detector. MAS NMR spectra were recorded at room temperature with a Bruker AV 400 spectrometer. ^{13}C cross-polarization (CP) MAS NMR spectra were recorded at a sample spinning rate of 5 kHz. ^{29}Si MAS NMR spectra were recorded with a spinning rate of 5 kHz at 79.459 MHz with a 55° pulse length of 3.5 μs and repetition time of 180 s. ^{29}Si and ^{13}C chemical shifts were referenced to tetramethylsilane and adamantane, respectively. ^{19}F MAS NMR spectra were measured at 376.28 MHz using a Bruker probe with 2.5 mm diameter zirconia rotors spinning at 25 kHz. The ^{19}F spectra were collected using pulses of 4.5 μs corresponding to a flip angle of $\pi/2$ rad and a recycle delay of 100 s to ensure the complete recovery of the magnetization. Thermogravimetric analyses were performed in an alumina pan with a TA Instruments device (SDT Q600) by increasing the temperature under flowing N_2 from ambient to 900 °C at a heating rate of 10 °C·min^{-1}. The organic content of the as-made materials was determined by elemental analysis in a SCHN FISONS elemental analyzer. A UV-Vis Cary 5 spectrometer equipped with a diffuse reflectance accessory was used for UV-Vis spectroscopic measurements. FTIR spectra were acquired with a Nicolet 710 spectrometer with 4 cm^{-1} resolution. The chemical analyses were carried out in a Varian 715-ES ICP-Optical Emission Spectrometer, after dissolution of the solids in an HNO_3/HCl/HF aqueous solution. Scanning electron microscopy (SEM) was performed using a Hitachi TM3000 TableTop microscope.

2.4. Computational details

The location and interaction energy of the 1B3MI cation in MFI were studied by molecular mechanics simulation, as implemented in Forcite module in Materials Studio software [35]. The molecular structure and interaction of the cations was modelled using the cvff forcefield [36]. Periodic boundary conditions (PBC) were applied in the calculations. The atomic charge distributions of the organic imidazolium cations were obtained from DFT calculations, using the B3LYP hybrid functional and the ESP charge calculation method, setting the total net charge to +1. The positive charge of the organic SDA molecules was compensated by reducing the Si charge from 0.6 until charge neutrality. Framework oxygen charges were kept fixed to −0.3. 1x1x1 unit cells MFI systems were used for the calculations, since this is large enough to avoid computational artefacts.

Initially, the 1B3MI imidazolium cations were manually located into the MFI zeolite framework; the most stable location of the OSDAs were obtained by Simulated Annealing calculations, where

the system is heated from 300 to 700 K and then down to 300 K with temperature increments of 20 K. 500 MD steps (NVT ensemble) of 1.0 fs were run on each heating step. This heating-cooling cycle was repeated for 10 times. The geometry of the system was optimized in each cycle and the system with the lowest interaction energy is chosen. Finally, the interaction energy was calculated by subtracting the energy of the 1B3MI OSDA in vacuum from the total energy.

3. Results and discussion

Table 1 summarizes the conditions and outcomes of the syntheses performed in this work. The 1B3MI cation led to two distinct zeolite phases (TON and MFI) depending on the synthesis conditions. It is worth mentioning that the range of H_2O/SiO_2 molar ratios investigated in this study (7–14) was selected based on previous reports of synthesis of zeolites in fluoride media using imidazolium cations as OSDAs [17].

As seen in Table 1, a pure silica TON zeolite crystallized under the conditions of synthesis A in the range of reaction times investigated (4–13 days). Nonetheless, the crystallinity of the TON sample significantly increased with increasing the synthesis time from 4 to 13 days, as inferred from the intensity of the reflections in the respective X-ray diffraction (XRD) patterns (Fig. 1a).

The use of seeds to induce the crystallization towards a specific structure is a common practice in zeolite synthesis [2,37]. Hence, an amount of 2 wt% (with respect to the weight of silica) of pure silica TON seeds was added to the gel mixture in synthesis B (H_2O/SiO_2 molar ratio of 14) in an attempt to drive the crystallization towards the formation of Ti-TON. Unfortunately, these synthesis conditions failed to yield a crystalline material even after 15 days of reaction as only the reflections related to the TON zeolite seeds were observed in the corresponding X-ray diffractograms (not shown). In syntheses C and D we reduced the H_2O/SiO_2 molar ratio from 14 to 7. In both cases, the use of a more concentrated gel led to the crystallization of the MFI phase for the investigated synthesis times (13–31 days), as shown in Table 1. The XRD patterns for the as-made MFI samples obtained in synthesis C (sample C-18) and in synthesis D after 13 days of synthesis (sample D-13) are shown in Fig. 1b. As observed, the addition of H_2O_2 to the gel in synthesis C to prevent anatase formation did not apparently influence the crystalline phase of the obtained zeolite. The fact that only the MFI phase crystallized under the conditions of syntheses C and D can be accounted for by considering the so-called Villaescusa's rule [38], according to which more concentrated gels tend to drive the crystallization toward less dense zeolite structures. Therefore, the more porous MFI phase (framework density of 17.9 T/1000 $Å^3$) was favored against the denser TON phase (framework density of 19.7 T/1000 $Å^3$) when the H_2O/SiO_2 molar ratio was reduced from 14 to 7 in syntheses C and D. The same behavior was observed in a previous study when the H_2O/SiO_2 molar ratio in the gel was decreased from 8.5 to 3.5 using 1-ethyl-3-methylimidazolium (1E3MI) cation as OSDA in the presence of HF [16]. In that work, the MFI phase was seen to be metastable and transformed into the more stable TON structure by the Ostwald ripening mechanism with increasing the crystallization time [16]. This behavior was, however, not observed here as MFI was the only crystalline phase obtained even after 31 days of synthesis (Table 1). On the other hand, in the work by Rojas et al. [16] TON zeolite was seen to be the favored phase at H_2O/SiO_2 molar ratios of around 7 using different doubly charged bis-methylimidazolium cations as OSDA. In contrast, in the present work MFI was the only crystalline phase obtained with 1B3MI at the H_2O/SiO_2 molar ratio of 7 (syntheses C and D), indicating that the chemical structure of the imidazolium OSDA might play a marked role in directing the crystallization toward a specific zeolite topology. Note, however, that in Ref. [16] the syntheses were carried out at a slightly lower temperature (150 °C) and under rotation. In our case, the fact that 1B3MI has rotation centers C-C-C and N-C-C in the lateral chain, allowing the molecule to adopt different conformations, could be considered an important factor driving the synthesis toward the more open MFI structure.

Next, the chemical, structural, and morphological properties of the as-synthesized TON and MFI zeolites are discussed based on different characterization techniques.

Table 2 collects information on the chemical composition of the as-synthesized materials. The experimental C/N atomic ratio in the as-made zeolites (around 4) agreed well with the theoretical value of 4.0 expected for the $1B3MI^+$ cation, which suggests that the OSDA should be occluded intact within the pores. Nevertheless, the presence of small amounts of decomposed products in the final solid cannot be discarded at this point. C analyses gave organic contents of 8.3% for TON sample A-13, and 11.4 and 11.6% for MFI samples C-18 and D-13. Thermogravimetric analyses (Fig. S1) were performed to determine the number of 1B3MI cations per unit cell. In the case of the pure silica TON, the obtained value of ~1 cation per unit cell (Table 2) is in fair agreement with that reported by Wen et al. [19], who noted that the size of 1B3MI (1 nm along the alkyl chain direction) is consistent with the unit cell size of TON. The OSDA packing for Ti-MFI (sample D-13) was found to be ~5 1B3MI cations per unit cell (Table 2). The difference between the OSDA packing for both zeolites can be related to the volume of unit cell, which is 5211.28 $Å^3$ and 1322.73 $Å^3$ for MFI and TON, respectively. The atomic Si/Ti ratio in the as-synthesized Ti-containing MFI samples (C-18 and D-13) was determined to be 150 and 145, respectively, roughly corresponding to two titanium atoms per three MFI unit cells (Table 2). This value is significantly lower than that in the synthesis gel (Si/Ti = 50), indicating an incomplete incorporation of Ti species in the solid. This behavior has been already noticed in the fluoride-mediated synthesis of titanosilicates, and was explained by the formation of a complex between titanium species and fluoride that prevented its effective incorporation in the zeolite framework [39].

The ^{13}C CP-MAS NMR spectra of the as-made TON (sample A-13) and Ti-MFI (sample D-13) zeolites (Fig. 2) show the characteristic resonances for $1B3MI^+$ cations, thus adding evidence to the presence of intact imidazolium moieties within the zeolite channels, as

Table 1
Summary of synthesis conditions and the resulting phase product.

Synthesis	$(Si/Ti)_{gel}$ ratio	H_2O/SiO_2 molar ratio	H_2O_2[a]	Seeds (wt%)[b]	Time (days)	Phase
A	∞	14	–	–	4, 5, 13	TON
B	50	14	–	2	4, 8, 15	Amorphous
C	50	7	Yes	–	18	MFI
D	50	7	–	–	13, 31	MFI

[a] SiO_2/H_2O_2 molar ratio = 0.333.
[b] Referred to the weight of silica.

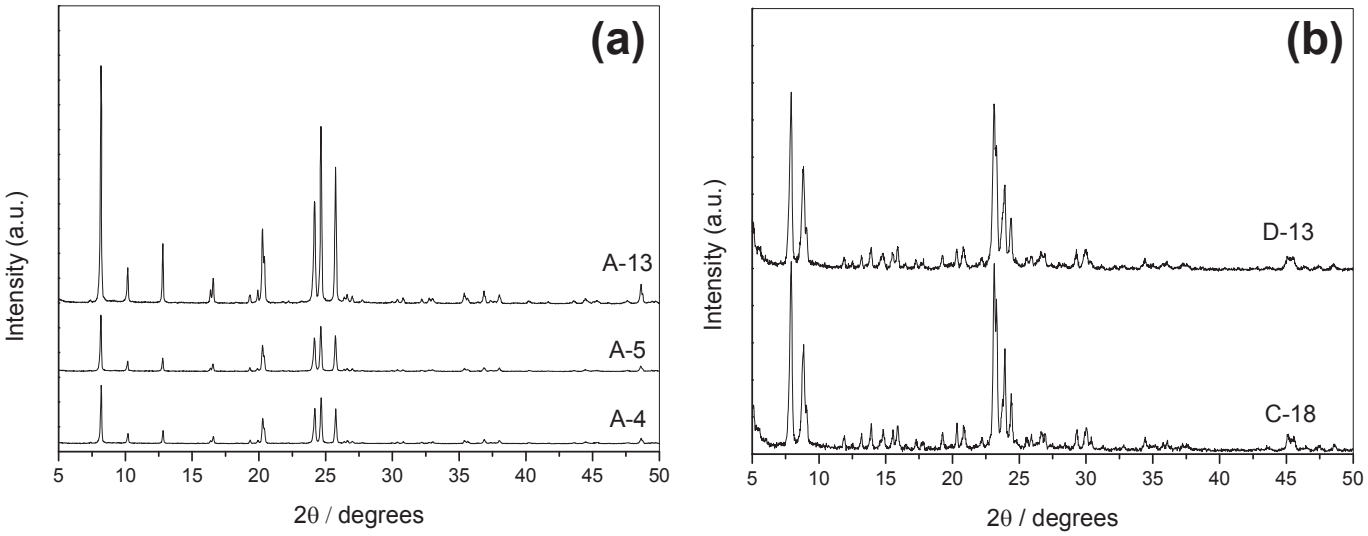

Fig. 1. X-ray diffraction patterns of as-made zeolites: (a) TON – samples A-4, A-5, and A-13; (b) MFI – samples C-18 and D-13.

Table 2
Chemical composition of the as-made TON and MFI zeolites.

Sample	Si/Ti_{exp}[a]	% C	% N	C/N[b]	Ti/u.c.	BMI^+/u.c.
A-13	∞	5.709	1.705	3.90	–	0.90
C-18	150	7.890	2.153	4.27	~2 Ti/3 u.c.	N.D.[c]
D-13	145	7.982	2.279	4.08	~2 Ti/3 u.c.	5.19

[a] Si/Ti atomic ratio determined from ICP-OES chemical analysis.
[b] C/N atomic ratio obtained by elemental analysis.
[c] Not determined.

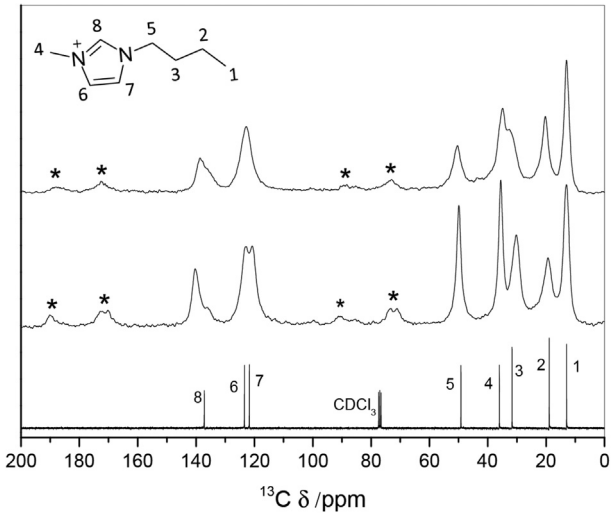

Fig. 2. ^{13}C CP-MAS NMR spectra of pristine 1-butyl-3-methylimidazolium (bottom), pure silica TON sample A-13 (middle), and Ti-MFI sample D-13 (top). Rotation bands are indicated with '*'.

suggested previously based on elemental analysis (Table 2). The resonances related to TON zeolite appear better resolved than those of MFI, pointing to a more heterogeneous environment for the imidazolium cations within the MFI channels [16] and/or to a higher mobility of the imidazolium cations in the TON framework. This should be expected due to the one-dimensional nature of the TON channels with a high degree of motion for the molecules, in contrast to MFI where the presence of the channel intersections probably reduces the molecular motion [40].

The environment for Si and F species in the as-made zeolites has been assessed by ^{29}Si and ^{19}F MAS NMR, respectively. The ^{29}Si MAS NMR spectra of the as-made TON (bottom) and Ti-MFI (top) samples showed two main resonances (Fig. 3a). The most prominent one, in the range of −108/−125 ppm, is related to Q_4 species, i.e., Si in a $Si[OSi]_4$ environment, while the small and broad resonance in the −95/−105 region is assigned to Q_3 sites, i.e. connectivity defects such as $Si[(OSi)_3O]^-$ or $Si[(OSi)_3OH]$. Deconvolution of the ^{29}Si MAS NMR spectra (not shown) indicated that around 3.1% of the Si atoms in TON (corresponding to ~0.7 SiO^- or SiOH/u.c.) and 1.8% of the Si atoms in MFI (corresponding to ~1.7 SiO^- or SiOH/u.c.) were involved in Q_3 environments.

On the other hand, the ^{19}F MAS NMR spectra for the as-made TON (bottom) and Ti-MFI (top) zeolites are presented in Fig. 3b. The MFI sample features a main resonance at around −69 ppm along with an additional, less intense, resonance at −81 ppm, indicating two different chemical environments for the fluoride anions in the zeolite micropores. Differently, MFI synthesized with TPA^+ and fluoride anions typically features a single ^{19}F resonance at around −69 ppm that has been unambiguously related to F ions located in a $[4^15^26^2]$ cavity of the zeolite framework [41]. As in the present work, Rojas et al. [16] did also observe two ^{19}F resonances at around −66 (much more intense) and −79 ppm in a pure silica MFI sample synthesized in fluoride media using 1-ethyl-3-methylimidazolium (1E3MI) as OSDA. The two ^{19}F NMR signals were associated to F atoms interacting with the 1E3MI cations in two different orientations, with the imidazolium ring located at the channels intersections. Given the similarity between the imidazolium molecules used as OSDA in Ref. [16] and in the present study and the similar position and relative contributions of the two ^{19}F NMR resonances, we speculate a similar location for the OSDA cations in the MFI sample synthesized in the 1B3MI-fluoride system. In the case of TON spectrum, a resonance around −76 ppm is observed, characteristic of fluoride in cavities of high silica zeolites (−38 to −80 ppm) [42].

The insertion of Ti in the MFI framework was assessed for the D-13 sample by means of IR and DRS UV-Vis spectroscopies. The IR

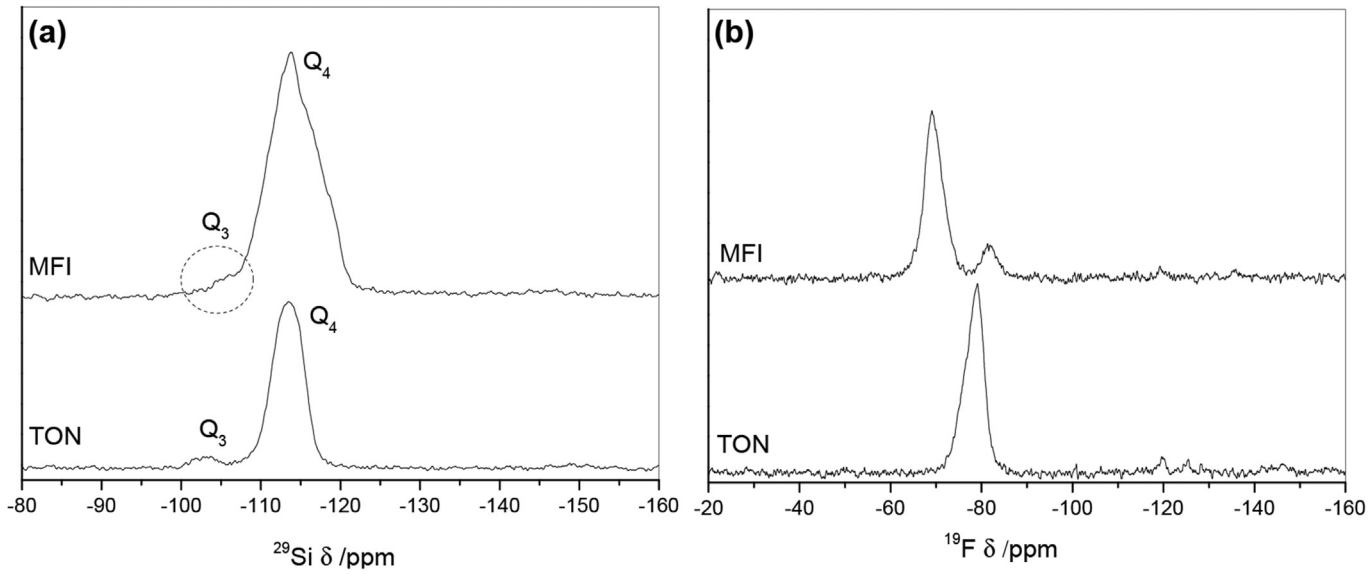

Fig. 3. ^{29}Si MAS NMR (a) and ^{19}F MAS NMR (b) spectra of as-made pure silica TON (sample A-13, bottom) and Ti-MFI (sample D-13, top).

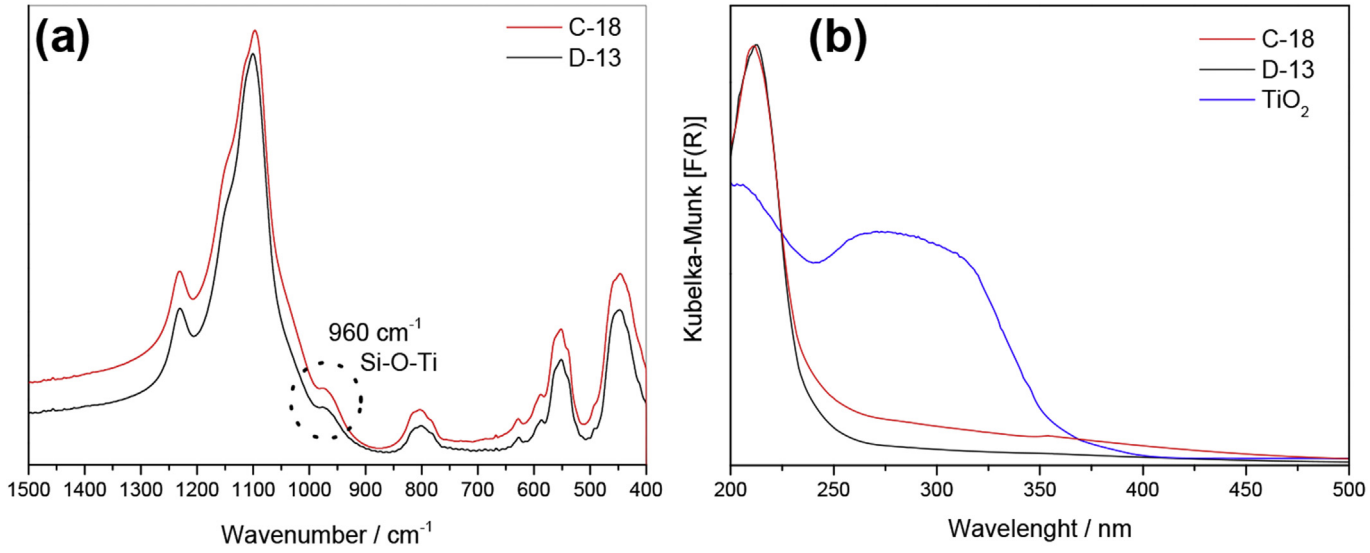

Fig. 4. Infrared (a) and diffuse reflectance UV-Vis (b) spectra of Ti-MFI zeolite (sample D-13).

band at ca. 960 cm^{-1} observed in Fig. 4a has been generally interpreted as the stretching vibration of framework [SiO_4] units perturbed by the presence of Ti [43]. In turn, the single band peaking at 200–220 nm evidenced in the DRS UV-vis spectrum (Fig. 4b) originates from the charge transfer between tetrahedrally coordinated titanium and oxygen and is widely taken as a fingerprint for the location of Ti species in the zeolite framework [10,43]. Therefore, both IR and DRS UV-vis spectroscopic measurements provide support for the presence of Ti species in the framework of the as-made Ti-MFI (sample D-13). Finally, it is worth mentioning that the absence of bands at wavelengths above 300 nm indicates, within the limits of the technique, that no extraframework anatase was present in our as-made Ti-MFI sample. The addition of hydrogen peroxide in the synthesis C-18 in comparison with synthesis D-13 seems to not have influence in preventing anatase formation, since both gel compositions do not led to extraframework TiO_2.

Finally, the morphology of the obtained TON and MFI zeolites was studied with SEM (Fig. 5). The TON zeolite (a-b) presents a morphology consisting of elongated rods with average size of approximately 40 μm. This morphology is characteristic of one-dimensional zeolites [44], while large crystallites are common for zeolites synthesized in fluoride media [2]. Distinctly, the MFI zeolite presents aggregates of crystals with regular size (smaller than 10 μm) similar to flower petals. These morphologies for MFI and TON synthesized in fluoride media using the 1-butyl-3-methylimidazolium as OSDA are quite different in comparison with those obtained in hydroxide media by our group in previous works [10,12], in which TON zeolite presented a homogenous morphology with form of grains of rice and particle size in the

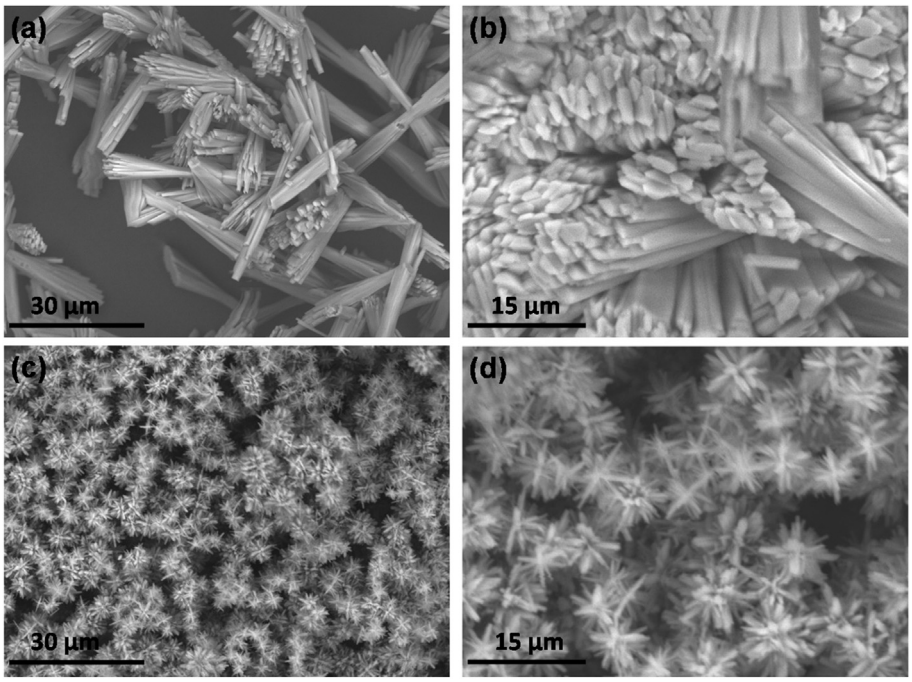

Fig. 5. SEM micrographs of as made pure silica TON (a-b, sample A-13), and Ti-MFI (c-d, sample D-13) zeolites.

Table 3
Interaction energies of different arrangement for 4 1B3MI-MFI molecules in one MFI unit cell, studied by Molecular Mechanics Calculations.

Entry	Imidazolium Location	Aliphatic Chain Location	E[a]
1	Intersection [010]	Straight [010]	−323.8
2	Intersection [010]	Sinusoidal [100]	−328.2
3	Sinusoidal [100]	Intersection [010]	−307.6

[a] Interaction Energy (kcal/mol per u.c).

5–30 µm range [10], whereas MFI zeolites are obtained in the form of regular microspheres [12]. The same morphology for TON was already obtained in hydroxide media using another OSDA [45].

In order to determine the location and interaction energy of the 1B3MI cations within the MFI structure, a computational study based on molecular mechanics was performed. We used a packing value of 4 cations per unit cell, and a primitive MFI unit cell. Initially, the cations were introduced manually into the MFI framework in the required orientation, obtaining the energy interactions and the most stable location of the organic OSDA by simulated annealing calculations. Table 3 shows the interaction energies of the 3B1MI cations within the MFI framework. Three different organic arrangements have been studied: with the imidazolium rings in the intersections between both channels, and the butyl chain in the straight (entry 1, Fig. 6-top) or in the sinusoidal (entry 2, Fig. 6-middle) channels, and with the imidazolium rings in the sinusoidal channels and the butyl chain in the channel intersections (entry 3, Fig. 6-bottom). Results of the interaction energies clearly shows that the location of the imidazolium rings is much more stable in the channel intersections (entries 1 and 2) than in the sinusoidal channels (entry 3, with an interaction energy of −307.6 kcal/mol), being the energy different of more than 15 kcal/mol (Table 3). This is probably due to the larger size of the channel intersections to host the bulky imidazolium rings. On the other hand, the butyl chains are slightly better accommodated when they site in the sinusoidal channels (with an interaction energy of −328.6 kcal/mol) than when they locate in the straight channels (−323.8 kcal/mol), which is probably a consequence of the more tight fitting of the butyl chain with the sinusoidal channels resulting in a stronger confinement effect. In sum, our computational study suggests that the most stable location for the 1B3MI cations involves siting the imidazolium rings on the channel intersections, and the butyl chains on the sinusoidal channels, although the difference in stability with siting the butyl chain in the straight channels is not very high, and therefore this could also occur during the crystallization process. Indeed, the potential occurrence of the two orientations for the butyl chains of the cation siting the imidazolium rings on the channel intersections could be related to the two different ^{19}F NMR signals of different intensity experimentally observed. This arrangement of the imidazolium cations where the ring locates in the channel intersections of the MFI framework is similar to the one we predicted in a previous work for 1,2,3-triethyl-imidazolium cations [40], suggesting that this ring strongly directs this zeolite building unit.

4. Conclusions

In the present study we have shown that the 1-butyl-3-methylimidazolium (1B3MI) cation exhibits different phase selectivity during the synthesis of zeolites in fluoride media depending on the conditions, and more specifically, on the gel concentration. Thus, TON was the only crystalline phase obtained in the synthesis of pure silica zeolites at a H_2O/SiO_2 molar ratio of 14. Attempts to produce Ti-TON, a novel titanosilicate, failed under these diluted conditions even when seeds of pure silica TON were added to the gel to induce the crystallization toward this topology. On the other hand, decreasing the H_2O/SiO_2 molar ratio from 14 to 7 selectively produced highly crystalline Ti-MFI, though only part of the Ti species were effectively incorporated to the solid, as inferred from the higher Si/Ti atomic ratio in the as-made material (Si/Ti = 142) compared to the synthesis mixture (Si/Ti = 50). Ti atoms were seen to be incorporated in the zeolite framework with no signs for extraframework TiO_2 (anatase) species, as corroborated by IR and

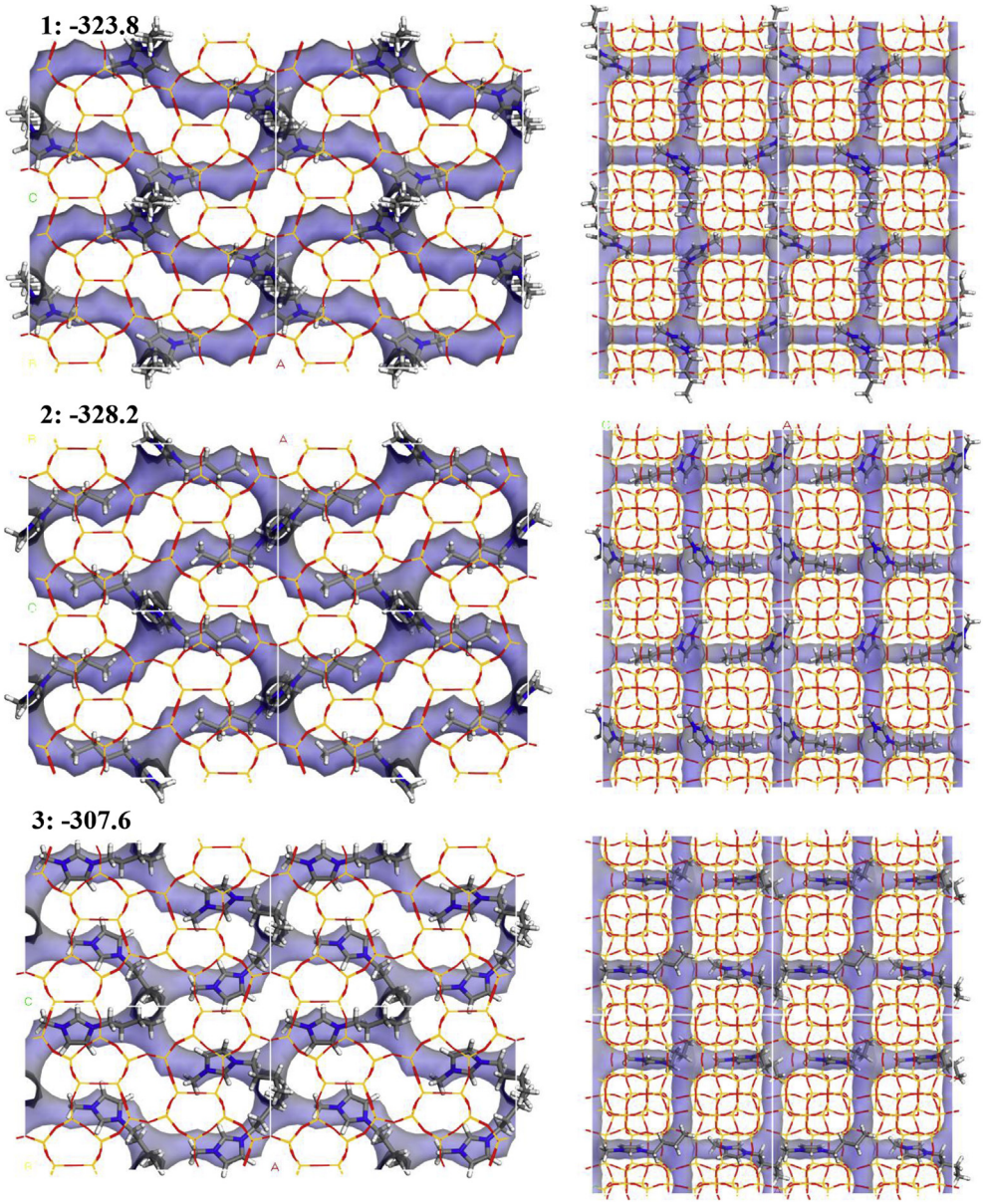

Fig. 6. Final location of 1B3MI cations in MFI with four SDAs per unit cell (Entries as reported in Table 3).

DRS UV-vis spectroscopies. The 1B3MI cations were confirmed to remain intact within the micropores by elemental analysis and ^{13}C CP-MAS NMR. Packing of the OSDA in the as-synthesized samples was calculated to be about 1 and 5 molecules per unit cell for pure silica TON and Ti-MFI, respectively. A small concentration of defects (as expected for fluoride-mediated syntheses) of 3.1% for TON and 1.8% for Ti-MFI was inferred from deconvolution of the respective ^{29}Si MAS NMR spectra. The molecular simulations showed that the most stable arrangement of the 1B3MI cations involves the location of the imidazolium rings on the channel intersections and of the butyl chains on the sinusoidal channels.

Acknowledgements

The authors gratefully acknowledge the Conselho Nacional de Desenvolvimento Científico e Tecnológico (CNPq) for financial support, and the Universidade Federal do Rio Grande do Norte (UFRN) for the physical structure. LGH acknowledges the Ministério de Economia y Competitividad of Spain for a Ramón y Cajal contract (RYC-2012-11794). Accelrys is acknowledged for providing the software, and Centro Técnico de Informática for running the calculations.

Appendix A. Supplementary data

Supplementary data related to this article can be found at http://dx.doi.org/10.1016/j.micromeso.2017.06.017.

References

[1] M. Moliner, F. Rey, A. Corma, Angew. Chem. Int. Ed. 52 (2013) 13880–13889.
[2] C.S. Cundy, P.A. Cox, Micropor. Mesopor. Mater 82 (2005) 1–78.
[3] B. Louis, L. Kiwi-Minsker, Micropor. Mesopor. Mater 74 (2004) 171–178.
[4] M.A. Camblor, A. Corma, P. Lightfoot, L.A. Villaescusa, P.A. Wright, Angew. Chem. Int. Ed. 36 (1997) 2659–2661.
[5] P.A. Barrett, M.A. Camblor, A. Corma, R.H. Jones, L.A. Villaescusa, Chem. Mater 9 (1997) 1713–1715.
[6] L.A. Villaescusa, P.S. Wheatley, I. Bull, P. Lightfoot, R.E. Morris, J. Am. Chem. Soc. 123 (2001) 8797–8805.

[7] M.A. Camblor, A. Corma, S. Valencia, J. Mat. Chem. 8 (1998) 2137–2145.
[8] A. Rojas, L. Gomez-Hortiguela, M.A. Camblor, Dalton Trans. 42 (2013) 2562–2571.
[9] R.H. Archer, S.I. Zones, M.E. Davis, Micropor. Mesopor. Mater 130 (2010) 255–265.
[10] C.W. Lopes, P.H. Finger, M.L. Mignoni, D.J. Emmerich, F.M. Teixeira Mendes, S. Amorim, S.B.C. Pergher, Micropor. Mesopor. Mater 213 (2015) 78–84.
[11] C.W. Lopes, J. Villarroel-Rocha, B.A. Da Silva, M.L. Mignoni, S.B.C. Pergher, Mat. Res. 19 (2016) 1461–1468.
[12] M.L. Mignoni, M.O. de Souza, S.B.C. Pergher, R.F. de Souza, K. Bernardo-Gusmão, Appl. Catal. A-Gen 374 (2010) 26–30.
[13] J.M. Martinez Blanes, B.M. Szyja, F. Romero-Sarria, M.A. Centeno, E.J. Hensen, J.A. Odriozola, S. Ivanova, Chem. Eur. J. 19 (2013) 2122–2130.
[14] D. Yuan, D. He, S. Xu, Z. Song, M. Zhang, Y. Wei, Y. He, S. Xu, Z. Liu, Y. Xu, Micropor. Mesopor. Mat. 204 (2015) 1–7.
[15] A. Rojas, O. Arteaga, B. Kahr, M.A. Camblor, J. Am. Chem. Soc. 135 (2013) 11975–11984.
[16] A. Rojas, L. Gomez-Hortiguela, M.A. Camblor, J. Am. Chem. Soc. 134 (2012) 3845–3856.
[17] A. Rojas, E. Martinez-Morales, C.M. Zicovich-Wilson, M.A. Camblor, J. Am. Chem. Soc. 134 (2012) 2255–2263.
[18] A. Rojas, M.A. Camblor, Chem. Mater 26 (2014) 1161–1169.
[19] H. Wen, Y. Zhou, J. Xie, Z. Long, W. Zhang, J. Wang, RSC Adv. 4 (2014) 49647–49654.
[20] M. Dodin, J.L. Paillaud, Y. Lorgouilloux, P. Caullet, E. Elkaim, N. Bats, J. Am. Chem. Soc. 132 (2010) 10221–10223.
[21] Y. Lorgouilloux, M. Dodin, J.-L. Paillaud, P. Caullet, L. Michelin, L. Josien, O. Ersen, N. Bats, J. Solid State Chem. 182 (2009) 622–629.
[22] P.A. Barrett, T. Boix, M. Puche, D.H. Olson, E. Jordan, H. Koller, M.A. Camblor, Chem. Commun. (2003) 2114.
[23] J.E. Schmidt, D. Xie, T. Rea, M.E. Davis, Chem. Sci. 6 (2015) 1728–1734.
[24] A. Rojas, M.A. Camblor, Angew. Chem. Int. Ed. 51 (2012) 3854–3856.
[25] A. Rojas, M.L. San-Roman, C.M. Zicovich-Wilson, M.A. Camblor, Chem. Mater 25 (2013) 729–738.
[26] D. Jo, S.B. Hong, M.A. Camblor, ACS Catal. 5 (2015) 2270–2274.
[27] R.E. Morris, Chem. Commun. (2009) 2990–2998.
[28] E.R. Parnham, R.E. Morris, J. Am. Chem. Soc. 128 (2006) 2204–2205.
[29] E.R. Parnham, R.E. Morris, Acc. Chem. Res. 40 (2007) 1005–1013.
[30] K.N. Marsh, J.A. Boxall, R. Lichtenthaler, Fluid Phase Equilib. 219 (2004) 93–98.
[31] T. Welton, Chem. Rev. 99 (1999) 2071–2084.
[32] J. Dupont, C.S. Consorti, P.A.Z. Suarez, R.F. de Souza, Org. Synth. 79 (2002) 236–243.
[33] H.G. Karge, J. Weitkamp, Synthesis - Molecular Sieves, first ed., Springer, 1998, pp. 187–228.
[34] G. Xiong, Y. Cao, Z. Guo, Q. Jia, F. Tian, L. Liu, Phys. Chem. Chem. Phys. 18 (2016) 190–196.
[35] Materials Studio™, Chem. Eng. News 78 (2000) (ibc).
[36] P. Dauber-Osguthorpe, V.A. Roberts, D.J. Osguthorpe, J. Wolff, M. Genest, A.T. Hagler, Proteins 4 (1988) 31–47.
[37] K. Iyoki, K. Itabashi, T. Okubo, Micropor. Mesopor. Mat. 189 (2014) 22–30.
[38] M.A. Camblor, L.A. Villaescusa, M.J. Díaz-Cabañas, Top. Catal. 9 (1999) 59–76.
[39] T. Blasco, M.A. Camblor, A. Corma, P. Esteve, J.M. Guil, A. Martínez, J.A. Perdigón-Melón, S. Valencia, J. Phys. Chem. B 102 (1998) 75–88.
[40] Y.M. Variani, A. Rojas, L. Gómez-Hortigüela, S.B.C. Pergher, New J. Chem. 40 (2016) 7968–7977.
[41] C.A. Fyfe, D.H. Brouwer, A.R. Lewis, J.-M. Chézeau, J. Am. Chem. Soc. 123 (2001) 6882–6891.
[42] M.A. Camblor, P.A. Barrett, M.a.-J. Díaz-Cabañas, L.A. Villaescusa, M. Puche, T. Boix, E. Pérez, H. Koller, Micropor. Mesopor. Mater 48 (2001) 11–22.
[43] A.M. Prakash, H.M. Sung-Suh, L. Kevan, J. Phys. Chem. B 102 (1998) 857–864.
[44] A.W. Burton, K. Ong, T. Rea, I.Y. Chan, Micropor. Mesopor. Mat. 117 (2009) 75–90.
[45] M.A. Asensi, A. Corma, A. Martínez, M. Derewinski, J. Krysciak, S.S. Tamhankar, Appl. Catal. A-Gen 174 (1998) 163–175.